International Journal of Communication Networks and Information Security
ISSN: 2073-607X, 2076-0930
Volume 15 Issue 03 Year 2023

Daily Activities of Elder Adults Using Optimized Deep Learning Model in China

Yun Yang
Ph.D. Candidate, Faculty of Built Environment,University Malaya, Kuala Lumpur, Malaysia, 50603
Director of Landscape Architecture Department, Faculty of Architecture, Chengdu College of Arts and Sciences, Chengdu, China, 610401
s2002999@siswa.um.edu.my
Nur Aulia Rosni*
Senior Lecturer, Faculty of Built Environment, University Malaya, Kuala Lumpur, Malaysia, 50603
nurauliarosni@um.edu.my
Rosilawati Binti Zainol
Associate Professor, Faculty of Built Environment, University Malaya, Kuala Lumpur, Malaysia, 50603
rosilawatizai@um.edu.my
Xiaohan Yang
Lecturer, Faculty of Environment and Art, TianFu College of SWUFE, Chengdu, China, 610052
adieyeung1122@126.com
Hang Hu
Associate Lecturer, Faculty of Architecture,Chengdu College of Arts and Sciences, Chengdu,China,610401
adahu97@163.com
Ting Wang
Associate Lecturer, Academic Affairs Office,Chengdu College of Arts and Sciences, Chengdu, China, 610401
cdwlddb@163.com

Article History

Received: 12 May 2023
Revised: 6 June 2023
Accepted: 13 July 2023

Abstract

The health and happiness of seniors can be influenced by the design of public spaces and buildings. Planning for age-friendly communities requires taking into account the wide variety of daily activities and public facility consumption among older persons. Yet, conventional approaches fall short when it comes to providing comprehensive, objective measures of the actions of the elderly. This research proposes an attention-based recognition approach by decomposing neural network outputs into class-dependent features using dictionary learning to improve discrimination performance. This research aimed to develop an empirical typology of activity of daily living (ADL) and its connection to health in China's ageing population. A deep learning-based model was rummaged to categorise the contributors in the Chinese Longitudinal Healthy Longevity Study (CLHLS) into subgroups based on their abilities with ADL. To be more precise, the study trains a category-based recognition network (CRN) by superimposing a basic but effective specific recognition encoding (SRE) unit on top of convolutional layers. In order to encode attention maps for each class, the SRE

module uses the feature maps produced by the Convolutional Neural Networks (CNN) to learn a class-specific vocabulary. Class-wise adaptive feature refining is achieved by multiplying these attention maps by the input features. In this case, a gazelle optimization algorithm (GOA) handles the hyper-parameter tuning process of the proposed model. This case study is the first of its kind in a dense metropolitan region, and it uses objective measurements to evaluate the activity spaces of the elderly. This research provides empirical data for the promotion of healthy ageing in urban areas.

Keywords: Activity of Everyday Living, Chinese Healthy Survey, Category-based Recognition Network, Gazelle Optimization Algorithm, Specific Recognition Encoding

1. Introduction

In 2016, it was estimated that 230 million people in China were 60 or older, making up 16.7% of the overall population [1]. One aspect of an ageing population is a rise in the sum of people who require long-term care as a result of many chronic circumstances and the treatment and consequences of those conditions. By 2020, it is projected that over 20 million China people and over will need some type of long-term care [2]-[4]. Due to the importance placed on filial piety in Chinese culture, home-based relaxed care has historically been the preferred method of long-term care in China [5]. A carer who places an elderly relative or other loved one in a long-term care facility (community, etc.) will be seen as disloyal. In addition, the problem is exacerbated by the fact that nursing facilities in China have traditionally been kept for persons who are childless, financially insecure, or have no living relatives [6]. Yet, due to population control measures taken in the 1970s, there are fewer family carers available to provide long-term care in the home. In particular, the current prevalence of "421/422" families places a heavy load on family informal carers [7], [8]. Furthermore, the lack of knowledge and training among relaxed carers [9], [10] presents additional difficulties.

There are a number of stressors associated with urban living, such as noise, air pollution, and crowding [11], that have been connected to a variety of negative public health consequences, with an increase in the risk of cardiovascular diseases and mental health issues [12]. One of the most often utilised criteria was the basic ADL (BADL) [13], which assesses fundamental capabilities including getting dressed, eating, and using the bathroom on one's own. The instrumental ADL (IADL) scale, developed by Lawton et al. [14] to evaluate ADL in the elderly, is a measure of how well an individual can adapt to their immediate surroundings in order to perform tasks like talking on the phone, going grocery shopping, preparing meals, and cleaning up after themselves. Given the strong association between BADL/IADL and functional ability, it was crucial to first determine the unique BADL/IADL profile in order to categorise the vast range of ageing populations in terms of their functional abilities [15]. Yet, prior research has shown that differentiating functional limitations in the elderly remains difficult and unclear due to overly broad categories or the excessive merging of evaluation elements [16]. An unsuitable definition of cut-points in an approximate scenario may contribute to the misclassification of functional limitation.

Efforts to solve these problems have persisted over many years. Previous research has examined visual attention in depth to determine its efficacy as a means of increasing the representational capacity of CNNs. Nevertheless, class-specific feature representations are rarely explicitly modelled by existing attention-based approaches. Class-specific representations can imprison and analyse the most vital data pertaining to an exact category and maintain enormous parting, so limiting attention to only those regions that are pertinent to the careful labels can yield performance improvements [17]. The study speculates that CNNs might be able to learn the ability to model class-specific representations if this is the case. The ability to learn feature representations that are unique to each class is a crucial step towards our aim. In recent years, numerous class-specific dictionary learning strategies have been investigated; in these approaches, each atom belongs to a particular class, and lexicon atoms belonging to various classes are fortified to be as autonomous as possible from one another.

Decoupling the semantic properties of the features is essential for encoding class-specific information. More recently, a number of strategies have been proposed to separate the characteristics that define each class from the others. Motivated by these education and class-specific techniques, this work suggests a dictionary-based CRN module in which each atom group stores a class-wise map containing clear class information. In the next step, the research integrates SRE into a CNN to create a fully functional CRN for the purpose of data recognition. It may direct the network to learn more judicial feature illustrations by using the SRE module to build class-specific attention maps. To ensure that the attention maps adequately reflect the various semantic classes, the study incorporates attention loss as a regularisation term during CRN training.

Overall, this study makes the following contributions:

(1) To ensure that the CNNs always encode class attention directly, the study proposes using the CRN module. To improve the CNN's discriminating capabilities, the CAE module can be easily integrated into existing models.

(2) As a means of extracting highly category-related feature representations, the work builds an end-to-end CRN using the SRE module and the corresponding attention loss.

(3) Many visual identification tasks, such as multi-label classification, are used to thoroughly test our approach. The experimental outcomes support the efficacy of the approach. The visualisation findings further show that class-specific dictionary learning allows CNN to explicitly learn class illustrations.

This paper's remaining sections are structured as follows. Initially, in Section 2, the existing research is studied and analyses the problem statement. Later, in Section 3, the proposed procedure is described in depth. The China dataset trials are then obtainable in Section 4. In Section 5, it concludes with paper's findings and recommendations.

2. Related Works

The 'Ensem-HAR' projected by Bhattacharya et al. [18] is a mixture of four different deep categorization models: the 'CNN-net,' Long Short-Term Memory Network (LSTM-net), 'ConvLSTM-net', and 'StackedLSTM-net'. The ensemble relies on a collection of categorization models that have a common foundation in 1D CNNs and LSTM networks but diverge in key architectural respects. When using the suggested Ensem-HAR for prediction, first stack predictions from the aforementioned four classification models, and then train a Blender or prediction to provide a final prediction for the test data. The suggested Ensem-HAR model for biomedical assessment was tested on three (WISDM, PAMAP2, and UCI-HAR), and it achieved 98.70%, accuracy, respectively. The new consequences demonstrate that the projected model outdoes the other numerous generated measurements that were used as comparisons. But, the model doesn't focus on the activity recognition of elder people and it doesn't focus on the China area.

The purpose of Garcia-Moreno et al [19].'s semi-automated gathering and investigation of health data to measure and forecast the dependency in older persons while performing one contributory living is to facilitate research and practise in this area. Here, examine whether the capture of data finished wearables during the completion of IADLs, with the use of learning algorithms, might substitute the outdated surveys used to measure requirements in a mobile-health scenario. To this goal, the study gathered information from wearables while elderly people went shopping. The acquired data was annotated by a trial supervisor (TC) with the various shopping stages (SS). Study utilised k-NN, RF, and SVM for our data pre-processing and analysis of these SS. The findings show that wearable data can successfully replace conventional questionnaires. In fact, the highest reported accuracy in determining dependency was 97% by the best learning methods tested. As a result of fine-tuning the algorithm's hyperparameters and employing an embedded feature selection strategy, the study was able to achieve optimal performance with a reduced set of only 10 features from an original collection of 85. This model solely takes into account information collected from a single wearable's accelerometer, activity, and temperature sensors. Despite the fact that these characteristics are not observable, the current concept is only because it requires a TS to name the SS. The work focused on shopping stage, whereas the proposed model focused on the indoor environment, especially for Chinese people.

A unified deep learning model is proposed by Alaghbari et al. [20] to track the progress of the elderly as they perform routine tasks including eating, sleeping, and taking medications. Activity detection and subsequent activity prediction are the components of the proposed method. A system like this can help seniors, their caretakers, and medical staff monitor patterns of behaviour and

develop interventions to address any issues that may arise. While each stage is often treated independently in the literature, our method builds on previous ones. After a deep neural network (DNN) is used to recognise activities based on various extracted features, an OCD-AE is used to distinguish between typical and unusual actions. At last, an LSTM algorithm is utilised to predict the next action based on a cleaned series of sequential actions. Given the importance of the activity recognition stage to the subsequent steps, the study proposes enhancing its precision by making use of several extracted features. The suggested unified approach's performance in recognising actions, detecting abnormalities, and predicting the next activity has been evaluated using real-world smart home datasets. The work focused on eating, sleeping and taking medicines alone elder people, however, the research work focused on more than three daily activities.

Chifu et al. [21] present a method for determining whether or not a senior's ADL monitoring data can be used to infer whether or not the senior needs assistance due to a change in their daily routine. Daily routines are identified using a Markov model-based method, with the entropy functions used to quantify and evaluate the degree of similarity between the observed routines. Beacons and trilateration methods form the basis of a decentralised monitoring system designed to track the whereabouts of the elderly. Positive findings include the ability to confidently identify daily routines with a confidence interval of [0.0794, 0.0829] for activity length and [0.0794, 0.0829] for activity sequence. When it comes to spotting outliers, our approach achieves an optimal sensitivity of 0.88 and an overall precision of 0.95.

Prenkaj et al. [22] as HypAD, and it is based on Anomaly Detection. HypAD utilises hyperbolic neural networks to provide end-to-end uncertainty estimation and incorporates this into the "traditional" idea of reconstruction loss in anomaly detection. HypAD is a novel principle that offers the concept of a detectable anomaly based on hyperbolic uncertainty. HypAD evaluates the input signal to determine if it is anomalous, for which case the model uncertainty would produce a high reconstruction loss, or if the signal is complex but regular, for which case the model uncertainty would generate a low loss. As part of a financed project including a multidisciplinary team of computer scientists, engineers, and geriatric specialists, the proposed method has been included in a monitoring scheme for senior patients in nursing homes. Credibility in the system was built by the participation of healthcare professionals in the design and verification processes. In addition, there are explanation mechanisms built into the system.

Patients in one Danish municipality who have trouble walking were monitored with accelerometers, and an (ML) based system was developed by Peimankar et al. [23]. The ML algorithm can reliably categorise the walking behaviour of people with a variety of walking disorders. Time series data was obtained using a sensor worn on the back of the individuals, and then various statistical, properties were retrieved from that data. Since individuals with dementia and disease may try to remove visible sensors to them, rear placement is preferable. Following this, a subset of features was chosen for inclusion in the classification process with the use of a PSO. With a dataset of 20 accelerometry readings, four different ML classifiers, including kNN, were trained and compared. The LOGO cross-validation (CV) method was used to assess these models. The Stack model had the highest performance, classifying walking episodes with averages of 86.85% sensitivity, 93.25% positive predictive values, 88.81% F1-score, and 93.32% accuracy. Empirical results generally supported the ability of the suggested models to classify the walking incidents, even with the difficult sensor assignment on the backs of patients with walking difficulties.

In order to detect falls and categorise different kinds of physical activity (PA), Chan et al. [24] offer a novel footwear strategy based on a CNN hybrid. Based on data from 32 subjects who individually performed PAs, it was shown that the detections employing deep-learning knowledge were effective: The F1-score for detecting falls with inertial measures was higher than for detection with foot pressures; the F1-score for detecting dynamic PAs (jump, jog, walks) was higher for inertial measures than for foot pressures; and the F1-score for detecting static PAs (sit, stand) was highest when using a combination of foot measures.

Kulurkar et al. [25] propose an innovative IoT-based system that uses low-power devices to detect falls of elderly people in indoor settings. For this, use a wearable sixLowPAN device equipped with a three-axis accelerometer to track the site and velocity of senior citizens in real time. With a sophisticated IoT gateway, the sensor's signals are analysed with a machine-learning model, resulting in superior fall detection accuracy. Here, employs inexpensive wearable sensing broadcast a design, and fall classification. Using set, which was built using the publicly available dataset "MobiAct," and analysed the optimal Nyquist rate, sensor location, and multiple channelling info

change. The edge computing solution uses analytics on data streams in real-time to identify falls with an accuracy of 95.87%.

The references from [21]-[25] are focused on elder people's activities with gait disorder or foot pressure and data are collected using wearable sensors and identified using Machine learning techniques or generic deep learning models. However the research work focused on class-specific modules and hyper-parameters are optimally selected by GOA.

3. Methodology

3.1 Data Source and Participants

Center for Healthy at Duke University oversaw the Chinese (CLHLS), which was approved out by the Chinese Center for Disease Control and Deterrence. There has been a total of eight data collection periods for the CLHLS: 1998 (baseline), the entire sample was recruited throughout 23 provinces comprising around 85% of China's total population. Hence, the CLHLS survey was considered the first biggest longitudinal survey of the aged in low- and middle-income nations [26]. For the CLHLS, researchers first found one eligible centenarian interviewee in the sampled city/county, and then they paired that person with another centenarian, an octogenarian, and three elders aged 65-79 who lived on the same street, hamlet, or town. To establish comparability with the randomly coded centenarians, the ages and sexes of participants aged 65-99 were predefined at random [27]. Health, both mental and access to medical treatment were among the topics covered in the CLHLS participants' surveys. Because of its high response rate, low missing data, and solid reliability/validity test findings, the CLHLS database was deemed to be of good quality [28]. CLHLS was described in further depth.

Participants in the 2018 wave of the CLHLS who were 65 or older were included in our analyses to ensure conformity with the most recent BADL/ IADL classifications for China's elderly population; however, dementia, or who were older than 105 were not. As a result, 8108 seniors were chosen for this investigation.

3.2 Assessment of BADL/IADL

The six domains that make up BADL were evaluated using the following scales: (1) bathing; (2) bandage; (3) toileting; (4) indoor movement. Respondents' levels of BADL reliance increased as their scores increased. The eight questions used to assess IADL included the following: (1) Can you visit your neighbours on your own? Can you (2) shop independently? Thirdly, you should be able to feed yourself in an emergency. The ability to do laundry independently is a requirement for point number four. Five) Are you able to walk a kilometre by yourself? Six) How about a 5-kilogram weight, like a full grocery bag? Can you perform three sets of continuous squatting and standing? Eight) Are you comfortable navigating the public transit system independently? The method used from 1 (total reliance) to 3 (full freedom) to rate each item (complete dependence). Respondents' functional dependency and subsequent requirements for personnel were directly correlated with their scores on the B- and I-ADL assessments. The capacity to perform both BADL and IADL independently has been shown to be a strong indication of functional disability in the elderly [29]. Moreover, Spector et al. stated that it would be viable and practical to include IADL in BADL persons in need of nursing. Functional impairment was indicated for participants when "full dependency" was recognised on BADL or IADL scales, and the 2018 CLHLS sample demonstrated.

3.3 Classification

As illustrated in Figure 1, the framework of our CRN has two primary sections. Specifically, (i) A module for encoding class attention mappings based on a learned dictionary for each class. Finally, the network is trained to acquire class-aware feature maps by encoding the attention maps into it. (ii) A novel regularisation term, called attention loss, to promote CRN for class-wise semantic information learning.

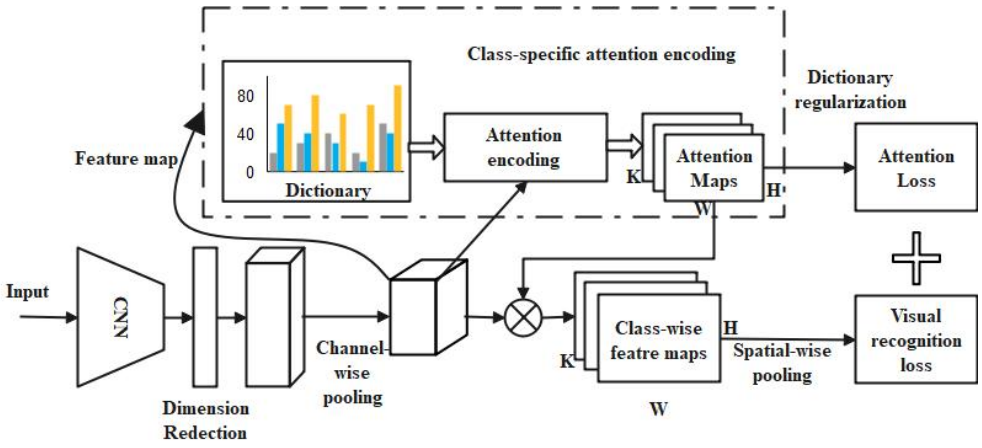

Figure 1. Architecture of CRN

A SRE module and the attention loss function are the backbone of the CRN. Attention mappings are encoded on a class-by-class basis in the SRE module. To help CRN learn class-wise semantic information more effectively, the study employs attention loss as a dictionary regularisation term. In total, a series of 11 convolutions is used to perform dimension reduction. The number of object classes is denoted by K, the number of atoms in the lexicon is denoted by N, and the dimension of an atom is signified by C.

3.3.1 Class-specific Dictionary

Many methods of credit are based on a synthesis lexicon that gives the illustrations of each data linear grouping of the dictionary. Input: a set of training data X, the lexicon learning can be expressed as:

$$\min_{D,z} \|X - DZ\|^2 \quad (1)$$

Where D is learned and Z contains the cargo constants.

In this study, a method that is organised by class is presented. Learning independent representations for each class is the underlying idea behind the class-specific dictionary. Let $D \in R^{C\times K\times N}$ represent a class-specific dictionary with K atom groups, N atoms per class, and C dimensions, where K is the sum of object groups, N is the sum of atoms in the dictionary and C is the sum of channels in the feature maps produced by CNN. It's significant to recall that the class semantic information is encoded in each atom group's attention map. As an added precaution, the training dispensation of the network should begin before the class-specific dictionary is established.

As shown in Figure 1, it employs distinct atomic groups to encode the data for each pixel vector in the maps, and then combine these maps to create K attention maps.

3.3.2 Attention Encoding

In order to make the most of the information for image identification despite the restrictions of GPU dimension decrease operation on the final convolution features using C 1×1 convolutions. As demonstrated in Figure 1, obtaining $X \in R^{C\times H\times W}$ serves as input to the SRE module. In this case, H and W stand for the height and breadth of the feature maps, respectively, and C is often significantly lower than the channel sum of the previous convolution topographies. It is possible to determine the degree of similarity between a set of C-dimensional pixel vectors, $x_C \in R^C$, and a set of atom vectors using the dictionary for that.

Suppose $D = \{d_l \in R^C | l = 1, \ldots, K \times N\}$ is the gathering of $K \times N$ atoms, where d_l is an dictionary. For the scheming of their similarity is expressed as:

$$S_{il} = \sigma(x_i, d_l) \quad (2)$$

Where $\sigma(\cdot)$ stands for a kernel function. In this case, the reaction of the lth pixel vector x_i to the lth atom vector d_l is denoted by a_{il}. Thus, a_{il} can be formulated as follows:

$$a_{il} = \frac{\sigma(x_i,d_l)}{\sum_{j=1}^{K\times N}\sigma(x_i,d_l)} \quad (3)$$

In order to avoid this, the dot kernel $a^{T}b$, (RBF) kernel $\exp(-\|a-b\|_2^2/\sigma^2)$, sigmoid kernel $\tanh(\beta a^{T}b+\theta)$, and so on. Seeing the competence, it accepts the internal dot kernel in exponential form. It is expressed as:

$$\sigma(x_i, d_l) = \exp(-d_l^{T}x_i) \tag{4}$$

And now, Equation (3) can be redeveloped into a more overall form:

$$a_{il} = \frac{\exp(-d_l^{T}x_i)}{\sum_{j=1}^{K\times N}\exp(-d_j^{T}x_i)} \tag{5}$$

Thus, using Equation (4) to analyze the reply for the maps. Let $A \in R^{K\times N\times H\times W}$ signify the got response media. The study behavior intra-group regular pooling process lengthways the (N) to get class-wise care maps $A^{att} \in R^{K\times H\times W}$. Let $a_{k,h,w}^{att} \in A^{att}$, which is shown as follows:

$$a_{k,h,w}^{att} = \frac{1}{N}\sum_{i=1}^{N} A_{k,i,h,w} \tag{6}$$

Notably, if the study directly multiplies $X \in R^{C\times H\times W}$ with the care matrix $A^{att} \in R^{K\times H\times W}$ to get the attention-guided maps, it computational difficulty and more GPU ingesting. To evade this problem, a channel-wise $X^{att} \in R^{K\times H\times W}$ by increasing $X' \in R^{1\times H\times W}$ with the care matrix $A^{att} \in R^{K\times H\times W}$, as exposed in Figure 1. The process can be expressed as

$$X_k^{att} = A_k^{att} \otimes X' \tag{7}$$

$$X^{att} = \mathrm{cat}(X_1^{att}, X_2^{att}, \ldots, X_K^{att}) \tag{8}$$

Where $A_k^{att} \in R^{H\times W}$ symbolizes the k-th $(k = 1, 2, \ldots, K)$ map fitting to the k-th class, $X_k^{att} \in R^{H\times W}$ denotes the k-th class, $\otimes$ signifies creation, and $\mathrm{cat}(\cdot)$ is a chain process. x feature maps $X^{att} \in R^{K\times H\times W}$ are class exact.

3.3.3 Training Loss

For the sake of optimization, it wants the attention map associated with an emerging class in an image to have a larger map. To help the SRE module and CRN learn class-wise semantic knowledge more effectively, the study incorporates a loss as a regularisation term. Specifically, it applies to maps, which is defined in Section 3.3.2 based on the symbol definition.$A^{att} \in R^{K\times H\times W}$ as shadows:

$$\begin{cases} v_k = \max_{i,j}(A_{i,j,k}^{att}) \\ v = (v_k)_{1\times K} \end{cases} \tag{9}$$

Where $v \in R^{K}$ is a chin used to calculate the loss. In brief, assumed dataset $\{I_i, y_i\}_{i=1}^{z}$, where I_i is the i-th image, $y_i = \{y_i^1, y_i^2, \ldots, y_i^K\}$ is its consistent vector. The consideration loss for a multi-label organization can be expressed as:

$$J_{att} = \sum_{i=1}^{Z}\sum_{j=1}^{K} y_i^j \log(v_i^j) + (1-y_i^j)\log(1-v_i^j) \tag{10}$$

Where v_i^j signifies the foretold likelihood of the i-th image fitting to the j-th group. As for classification, the courtesy loss is expressed as:

$$J_{att} = \sum_{i=1}^{Z}\sum_{j=1}^{K} y_i^j \log\left(\frac{v_i^j}{\sum_{j=1}^{K} v_i^j}\right) \tag{11}$$

J_{cls}, shorthand for the loss of visual recognition, varies between tasks. In this study, a variety of tasks is performed, both of which share loss. On the other hand, they calculate losses differently. Features extracted from class-specific attention maps are combined and used in the attention loss.$A^{att} \in R^{K\times H\times W}$ while class-wise feature maps are pooled to create a visual classification loss $X^{att} \in R^{K\times H\times W}$. The total loss can be characterised as follows, factoring in the decline in both visual recognition and focus:

$$J = J_{cls} + \lambda J_{att} \tag{12}$$

Where λ is the overall loss balancing coefficient. The performance of visual recognition tasks can be improved by jointly optimizing these two loss terms J_{cls} and J_{att}. In this case, GOA is used to fine-tune the suggested model's hyper-parameters, as explained below.

3.3.4 The Gazelle Optimization Algorithm (GOA)

The ability of GOA is to escape from local optima and perform exploitation and exploration, because they have only one global optimum. The popularity and success of proposing algorithms

that mimic the behaviors of animals to solve optimization problems with appropriate accuracy. The (GOA) is introduced, and an optimization strategy is developed, in this part. As the GOA is population-based, it can be used for any optimization issue.

3.3.4.1 Population Initialization

Optimization using the GOA kicks off with an initialization of the gazelle population (X) based on the Equation (13). Populations are created randomly among the upper bound (UB) and lower bound (LB) of the specified problem (LB).

$$X = \begin{bmatrix} x_{1,1} & x_{1,2} & \cdots & x_{1,d-1} & x_{1,d} \\ x_{2,1} & x_{2,2} & \cdots & x_{2,d-1} & x_{2,d} \\ \vdots & \vdots & x_{i,j} & \vdots & \vdots \\ x_{n,1} & x_{n,2} & \cdots & x_{n,d-1} & x_{n,d} \end{bmatrix} \quad (13)$$

Where X is the current collection of candidate populations (solutions), shaped accidentally using Equation (14), $x_{i,j}$ is the site of the ith population along the jth dimension, n is the total sum of populations (solutions), and d is the problem's dimension.

$$x_{i,j} = \text{rand} \times \left(UB_j - LB_j\right) - LB_j \quad (14)$$

Where $rand$ is a random number, UB_j and LB_j are a problem, respectively. Each iteration ends with an approximation of the optimal solution based on the best answer acquired so far. The fittest and healthiest gazelles, it is thought, are the best at spotting rewards, spreading the word to others, and escaping from predators. This means the most optimal answer is chosen as the "gazelle" to be used in the Elite matrix (Equation 15). The gazelles utilise this matrix to look up information and figure out what to do next.

$$\text{Elite} = \begin{bmatrix} x'_{1,1} & x'_{1,2} & \cdots & x'_{1,d-1} & x'_{1,d} \\ x'_{2,1} & x'_{2,2} & \cdots & x'_{2,d-1} & x'_{2,d} \\ \vdots & \vdots & x'_{i,j} & \vdots & \vdots \\ x'_{n,1} & x'_{n,2} & \cdots & x'_{n,d-1} & x'_{n,d} \end{bmatrix} \quad (15)$$

Where $x'_{i,j}$ represents the top gazelle vector, It is then used to create the Elite matrix by being copied n times. Both the predator and the prey can be thought of as search agents in this context. For the simple reason that the gazelles and the predator will be headed in the similar direction towards the safe haven by the time the gazelles have noticed the predator and taken off running, and the predator will have previously investigated the area by the time the gazelles have made their escape. If the top gazelle is replaced by a superior one, the Elite will be changed at the end of each cycle. A random process where the stepsize is selected from a Normal (Gaussian) distribution with a mean and standard deviation of zero and one, respectively. Standard Brownian motion [30] is defined by the equation:

$$f_B(x, \mu, \sigma) = \frac{1}{\sqrt{2\pi\sigma^2}} \exp\left(-\frac{(x-\mu)^2}{2\sigma^2}\right) = \frac{1}{\sqrt{2\pi}} \exp\left(-\frac{x^2}{2}\right) \quad (16)$$

Using the given by Equation 17 [30], the Lévy flight implements a random walk.

$$L(x_j) \approx \left[x_j\right]^{1-a} \quad (17)$$

Where x_j denotes the flight length and $1 < \alpha \leq 2$ represents the power-law advocate. Equation 18 denotes the Lévy stable procedure as an integral.

$$f_L(x; a, \gamma) = \frac{1}{\pi} \int_0^{\infty} \exp(-\gamma q^a) \cos(qx) \delta q \quad (18)$$

Where is the scale index that determines how the motion's scale is distributed, and is the scale unit. Our research took advantage of a method provided in [30] for generating a steady Lévy motion. The algorithm operates with values of between 0.3 and 1.99, as stated by Equation 19.

$$\text{Levy}(a) = 0.05 \times \frac{x}{|y|^{\frac{1}{a}}} \quad (19)$$

Where α, x and y are defined as follows:

$$\sigma_x = \left[\frac{\Gamma(1+a)\sin\left(\frac{\pi a}{2}\right)}{\Gamma\left(\frac{(1+a)}{2}\right) a 2^{\frac{(a-1)}{2}}}\right]^{\frac{1}{a}} \quad (20)$$

Where $\sigma_y = 1$, and $a = 1.5$.

The suggested GOA algorithm models gazelle survival behaviour including grazing while no danger is present and fleeing to safety when a predator is observed. As a result, the suggested GOA algorithm's optimization techniques are split into two distinct stages.

3.3.4.2 Exploitation

In this stage, the predator is either actively stalking the gazelles or has given up and the gazelles are contentedly grazing. To efficiently cover nearby regions of the domain, the study employed the Brownian motion, which is characterised by uniform and controlled steps. Brownian motion is used to characterise the gazelles' anticipated grazing behaviour. Equation 21 depicts the mathematical model of this behaviour.

$$\overrightarrow{\text{gazelle}}_{l+1} = \overrightarrow{\text{gazelle}}_l + s.\vec{R} * . \vec{R}_B * . \left(\overrightarrow{\text{Elite}}_l - \vec{R}_B * . \overrightarrow{\text{gazelle}}_l\right) \quad (21)$$

Where $\overrightarrow{\text{gazelle}}_{l+1}$ is the solution of the following iteration, $\overrightarrow{\text{gazelle}}_l$ is the key at the present iteration, s denotes the grazing haste of the gazelles, $\vec{R}_B$ is a vector covering chance statistics motion, R is a vector of unchanging accidental statistics in [0,1].

3.3.4.3 Exploration

After a predator is seen, the investigation phase begins. It modelled the gazelle's defensive behaviour, which consists of a tail flick, a stomp of the foot, or a "stotting" jump in which all four legs are planted at once at a height of 2 metres, by setting the height of the leap to a value between 0 and 1. At this point in the algorithm, the study employed the Lévy flight, which entails a sequence of little steps followed by larger ones every so often. It has been used to make optimization literature easier to find via a web search by employing this method. Figure 3 shows this process of discovery in its early stages. The gazelle sees the lion and takes off, and the lion gives pursuit. This represents the abrupt reversal in direction that characterises both runs. The study hypothesised that this reversal occurs at regular intervals, with the gazelle travelling in one direction when the iteration sum is odd and in the opposite direction when the iteration number is even. As the gazelle is quicker to act, the study reasoned that it must use Lévy flying when running. As the predator's reaction time is longer, it would use Brownian motion during its takeoff run before switching to Lévy flight. Once the gazelle detects the predator, its behaviour can be mathematically modelled using Equation 22.

$$\overrightarrow{\text{gazelle}}_{l+1} = \overrightarrow{\text{gazelle}}_l + S.\mu.\vec{R} * . \vec{R}_L * . \left(\overrightarrow{\text{Elite}}_l - \vec{R}_L * . \overrightarrow{\text{gazelle}}_l\right) \quad (22)$$

For the gazelle's top speed, S, the Lévy distribution notation for a vector of random values is used, $\vec{R}_L$. Equation 23 depicts the exact perfect for the behaviour of the predator pursuing the gazelle.

$$\overrightarrow{\text{gazelle}}_{l+1} = \overrightarrow{\text{gazelle}}_l + S.\mu.\text{CF} * . \vec{R}_L * . \left(\overrightarrow{\text{Elite}}_l - \vec{R}_L * . \overrightarrow{\text{gazelle}}_l\right) \quad (23)$$

Where $\text{CF} = \left(1 - \frac{\text{iter}}{\text{Max\_iter}}\right)^{\left(2\frac{\text{iter}}{\text{Max\_iter}}\right)}$ denotes the parameter that controls the movement of the predator In a study of Gazelles, While the authors acknowledge that gazelles are not in danger of extinction, they note that their rate of 0.66 indicates that predators are only successful in 0.34 of instances. The algorithm avoids being stuck in a local minimum by taking into account the predator success rates (PSRs), which in turn affect the gazelle's ability to escape. Equation 24 is a model for the influence of PSRs.

$$\overrightarrow{\text{gazelle}}_{l+1} = \begin{cases} \overrightarrow{\text{gazelle}}_l + \text{CF}\left[\overrightarrow{\text{LB}} + \vec{R} * . \left(\overrightarrow{\text{UB}} - \overrightarrow{\text{LB}}\right)\right] * \vec{U} & \text{if } r \le \text{PSRs} \\ \overrightarrow{\text{gazelle}}_l + [\text{PSRs}(1-r) + r]\left(\overrightarrow{\text{gazelle}}_{r1} - \overrightarrow{\text{gazelle}}_{r2}\right) & \text{else} \end{cases} \quad (24)$$

Where $\vec{U}$ signifies a binary vector, which is built by making a random sum in [0,1] such that $\vec{U} = \begin{cases} 0, & \text{if } r < 0.2 \\ 1, & \text{otherwise} \end{cases}$, r1, r2 are random matrix.

3.3.4.4 Computational Complexity

Typically, the computational difficulty of the GOA is based on the rules: solutions initialization and updating the solutions. Assuming there are n solutions, their initialization procedures have a computational complexity of $O(n)$. All solutions' updating operations, which include both searching for the optimal positions and updating the solutions' positions, have a computational complexity of $O(\text{iter} \times d) + O(CFE)$. Iteration count (iter), issue dimension (d), and function evaluation (CFE) cost. As such, the suggested GOA has a high computational complexity is $O(\text{iter} \times d \times n + CFE \times n)$.

Algorithm

begin
Initialize the algorithm parameters
s= [0, 1]
μ= [-1, 1]
S= 88kmph
PSRs=0.34
R and r are random numbers [0, 1]
Initialize the gazelle populations (search agents)
While iter<max_iter
Calculate the gazelles
construct the Elite gazelle matrix
If r<2
Update gazelles based on

$$\overrightarrow{\text{gazelle}}_{l+1} = \overrightarrow{\text{gazelle}}_l + s.\vec{R} * . \vec{R}_B * . \left(\overrightarrow{\text{Elite}}_l - \vec{R}_B * . \overrightarrow{\text{gazelle}}_l\right)$$

Else
If mod(iter,2==0)
μ = -1
Else
μ = 1
For the gazelle populations
Update gazelles based on

$$\overrightarrow{\text{gazelle}}_{l+1} = \overrightarrow{\text{gazelle}}_l + S.\mu.\vec{R} * . \vec{R}_L * . \left(\overrightarrow{\text{Elite}}_l - \vec{R}_L * . \overrightarrow{\text{gazelle}}_l\right)$$

For the predator populations ($i = n - 2, \ldots, n$)
Update gazelles based on

$$\overrightarrow{\text{gazelle}}_{l+1} = \overrightarrow{\text{gazelle}}_l + S.\mu.CF * . \vec{R}_L * . \left(\overrightarrow{\text{Elite}}_l - \vec{R}_L * . \overrightarrow{\text{gazelle}}_l\right)$$

End (if)
Elite update
Applying PSRs result and update based on

$$\overrightarrow{\text{gazelle}}_{l+1} = \begin{cases} \overrightarrow{\text{gazelle}}_l + CF\left[\overrightarrow{LB} + \vec{R} * . \left(\overrightarrow{UB} - \overrightarrow{LB}\right)\right] * \vec{U} & \text{if } r \leq PSRs \\ \overrightarrow{\text{gazelle}}_l + [PSRs(1-r) + r]\left(\overrightarrow{\text{gazelle}}_{r1} - \overrightarrow{\text{gazelle}}_{r2}\right) & \text{else} \end{cases}$$

End while
End

3.4 Coding of Rudimentary Features and Health Indicators

Classification was used to transform continuous variables, educational background, recent physical exercise (no=0, yes=1), recent social activities (no=0, yes=1), and location. Self-reports and objective measurements were used to collect health factors, such as body mass index and comorbidity status, as well as cognitive symptoms. The overall level of cognitive function was measured using the Mandarin translation of the Mini-Mental State Examination (MMSE). Higher

scores on the MMSE's 24 items (ranging from 0 to 30) imply greater reliance on the test-takers' part in the area of cognitive orientation, computation, recall, and language capacity. Scores of 24 or higher indicated "normal cognitive function" in the elderly, whereas scores below this threshold indicated "cognitive impairment" [31]. The depression symptom, which ranges from 0 to 30 and uses a cutoff score of 10 to differentiate between normal and depressive groups. Body mass index was determined by using the formula: (m2). Underweight individuals had a body mass index (BMI) of less than 18.5, whereas those with normal weight BMIs between 18.5 and 24 were considered neither overweight nor obese. Fall history and self-reported diagnoses of comorbidities like hypertension, diabetes and cardiovascular disease, were recorded.

4. Results and Discussion

Python 3.7.0 is used for our investigations, with the deep learning framework implemented in PyTorch 1.2.0. For our tests, the study had an RTX2060 GPU running on 6 GB of RAM and an AMD CPU running at 2.9 GHz on 16 GB of Memory. To implement the proposed network, ResNet-101 is used, since it is considered as a basic architecture and the stochastic gradient descent (SGD) is used as an optimizer to train the network. Initially, the momentum is set to 0.9 and the weight delay is 0.0003, where the GOA is applied to find the optimal solution for this hyper-parameter. Finally, the momentum is set to 0.7 and the weight delay is 0.0001. The learning rate is 0.05 for the class-specific attention encoding module and 0.005 for the backbone, the epoch is set to 50. Each GPU's batch size is 16 with 2 GPUs, then the learning rate is multiplied by a factor of 0.1 at the 12th, 25th, and 40th epochs. For GOA, the population size is set to 50 and the maximum number of iterations is set to 1000, finally, the independent runs for the algorithm are set to 30.

4.1 Performances Metrics

The accuracy (Acc), area under the curve, F1 score (F1) and average precision (AP) were utilised to gauge the efficacy of our model. Equation (25) can be used to determine the accuracy.

$$\text{Accuracy} = \frac{\text{TP+TN}}{\text{TP+TN+FP+FN}} \tag{25}$$

The precision is intended by the subsequent Equation (26):

$$\text{Precision} = \frac{\text{TP}}{\text{TP+FP}} \tag{26}$$

The recall is intended by the subsequent Equation (27):

$$\text{Recall} = \frac{\text{TP}}{\text{TP+FN}} \tag{27}$$

The F1 is intended by the subsequent Equation (28):

$$\text{F1} = 2\frac{\text{Precision}*\text{recall}}{\text{Precision+recall}} \tag{28}$$

The AUC curves evaluate the accuracy of a test by contrasting the proportion of correct predictions with the proportion of incorrect ones for various cutoff values. The precision-recall curve is summarised by AP as the weighted mean of accuracy at each threshold. The existing models with proposed model are tested and compared with various training and testing data ratios. The existing models use different datasets, therefore the generic models are considered and tested with our datasets, then the results are averaged in Table 1 to 3. The data plays a major role in the performance of the model, and in order to test the effectiveness of the model, the analysis is focused on 60%, 70% and 80% of training data with 40%, 30% and 20% of testing data, which is termed as k-cross validation analysis.

Table 1. Comparative Analysis of Proposed Model for 60%-40%

Model	Acc	AP	AUC	F1	Precision	Recall
LSTM	0.8346	0.8477	0.7572	0.8807	0.8284	0.8187
CRN	0.8478	0.8479	0.7590	0.8913	0.8263	0.8263
DBN	0.8477	0.7431	0.8745	0.8085	0.8210	0.7964
CNN	0.8479	0.7661	0.8651	0.8187	0.8362	0.7844
CRN-GOA	0.8688	0.7886	0.9058	0.8503	0.8503	0.8503

When the models are tested with accuracy, the proposed model achieved 0.86, and existing techniques achieved nearly 83% to 84%. The reason for better performance is that the CRN's hyper-

parameters are optimized by using GOA model. The existing models such as DBN, CNN, LSTM and CRN achieved nearly 87% to 89% of AUC, 80% to 82% of F1, 81% to 83% of precision, 79% to 83% of recall and 74% to 76% of AP. But the proposed model achieved 90% of AUC, 85% of F1, 85% of precision, 78% of AP and 85% of recall.

Table 2. Performance Analysis of Proposed Model with Existing Techniques for 70%-30%

Model	Acc	AUC	F1	Precision	Recall	AP
DBN	0.8482	0.8797	0.8095	0.8151	0.8041	0.7339
CNN	0.8451	0.8749	0.8162	0.8506	0.7844	0.7618
LSTM	0.8583	0.8787	0.8333	0.8599	0.8084	0.7791
CRN	0.8688	0.9058	0.8503	0.8503	0.8503	0.7886
CRN-GOA	0.8766	0.9135	0.8563	0.8750	0.8383	0.8044

In this analysis, the DBN reached the Acc of 0.8482, the AUC of 0.8797, the F1 score value of 0.8095, the precision value of 0.8151, the recall rate of 0.8041 and the finally AP value of 0.7339. CNN reached the Acc of 0.8451, the AUC of 0.8749, the F1 score value of 0.8162, 0.8506, 0.7844 and the finally AP value of 0.7618. LSTM reached the Acc of 0.8583, the AUC of 0.8787, the F1 score value of 0.8333, the recall rate of 0.8599 and AP value of 0.7791. CRN reached the Acc of 0.8688, the AUC of 0.9058, the F1 score value of 0.8503, the recall rate of 0.8503 and AP value of 0.7886. CRN-GOA reached the Acc of 0.8766, the AUC of 0.9135, the F1 score value of 0.8563, the recall rate of 0.8750 and finally AP value of 0.8044 respectively. The drawback of LSTM is that it requires more memory to train all the samples and leads to high memory consumption.

Table 3. Analysis of Proposed Model for 80%-20% of Training and Testing Data

Model	Acc	AUC	F1	Precision	Recall	AP
DBN	0.8482	0.8797	0.8095	0.8151	0.8041	0.7339
CNN	0.8241	0.8846	0.8069	0.7778	0.8383	0.7229
LSTM	0.8451	0.8649	0.8162	0.8506	0.7844	0.7618
CRN	0.8661	0.8904	0.8440	0.8625	0.8263	0.7888
CRN-GOA	0.8871	0.9088	0.8693	0.8827	0.8563	0.8189

In this analysis the DBN reached the Acc of 0.8482, the AUC of 0.8797, the F1 score value of 0.8095, the precision value of 0.8151, the recall rate of 0.8041 and the finally AP value of 0.7339. CNN reached the Acc of 0.8241, the AUC of 0.8846, the F1 score value of 0.8069 and the finally AP value of 0.72229. LSTM reached the Acc of 0.8583, the AUC of 0.8787, the F1 score value of 0.8333, the recall rate of 0.8599, the recall rate of 0.8084 and the finally AP value of 0.7791. CRN reached the Acc of 0.8661, the AUC of 0.9058, the F1 score value of 0.8503, the recall rate of 0.8503, the recall rate of 0.8503 and the finally AP value of 0.7886. CRN-GOA reached the Acc of 0.8766, the AUC of 0.9135, the F1 score value of 0.8563, the recall rate of 0.8750, the recall rate of 0.8563 and the finally AP value of 0.8189.

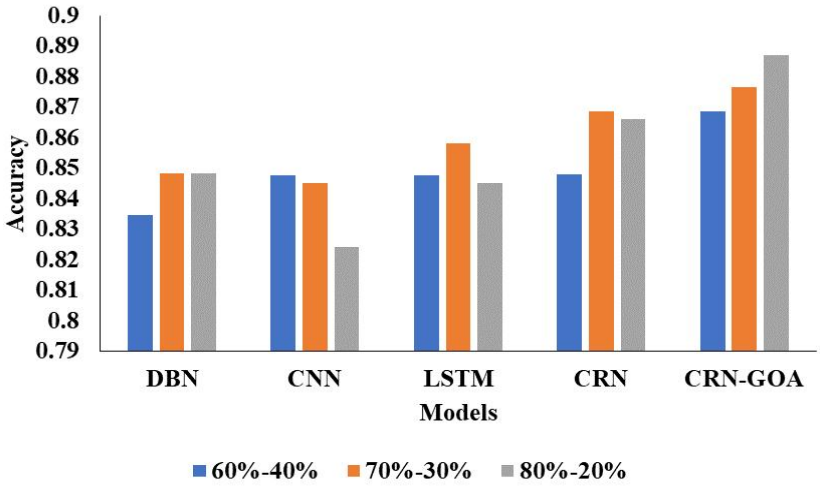

Figure 2. Performance Analysis of Proposed Model Using Accuracy

Figure 2 represents that the performance analysis of proposed model using accuracy. In this analysis, we take different datasets to split up and compared different techniques. By this comparison analysis, the proposed model reaches better results respectively.

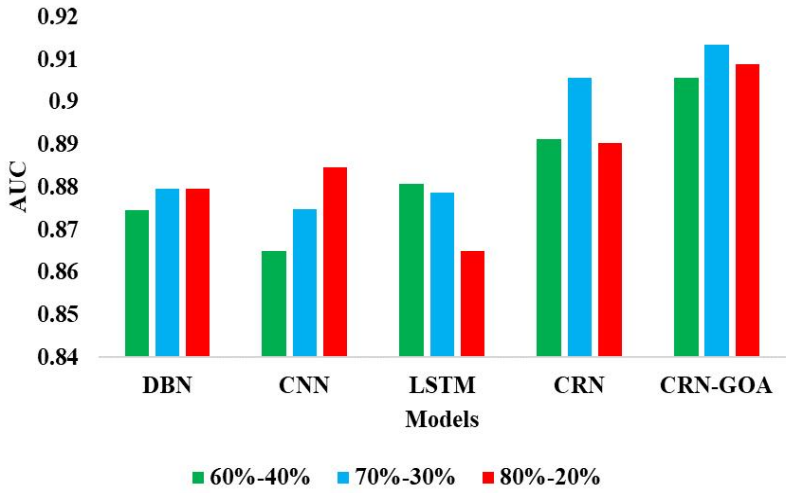

Figure 3. AUC Comparison

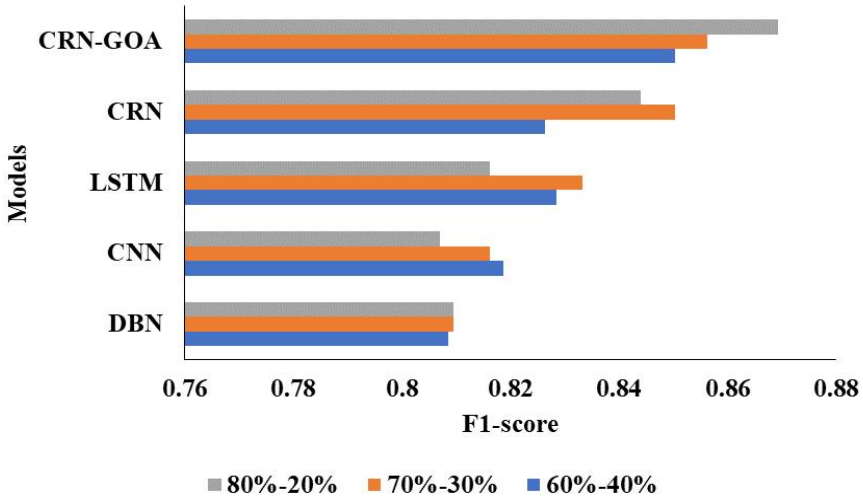

Figure 4. F1-score Comparison

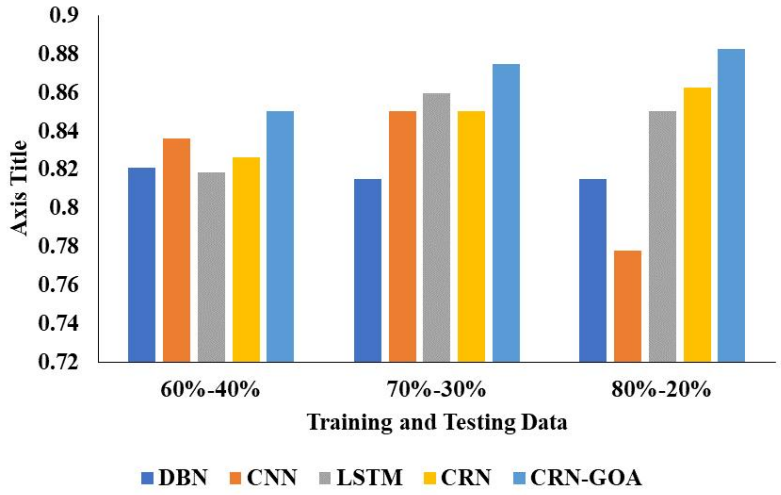

Figure 5. Precision Validation Analysis of Various Techniques

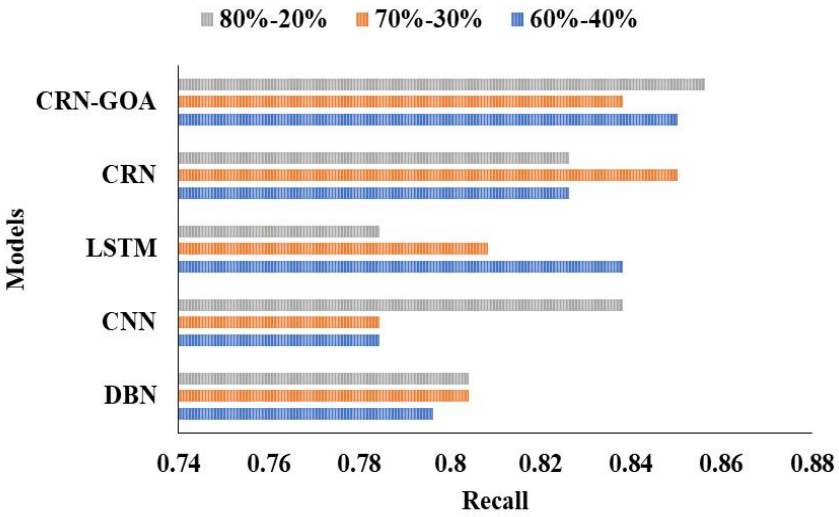

Figure 6. Recall Analysis

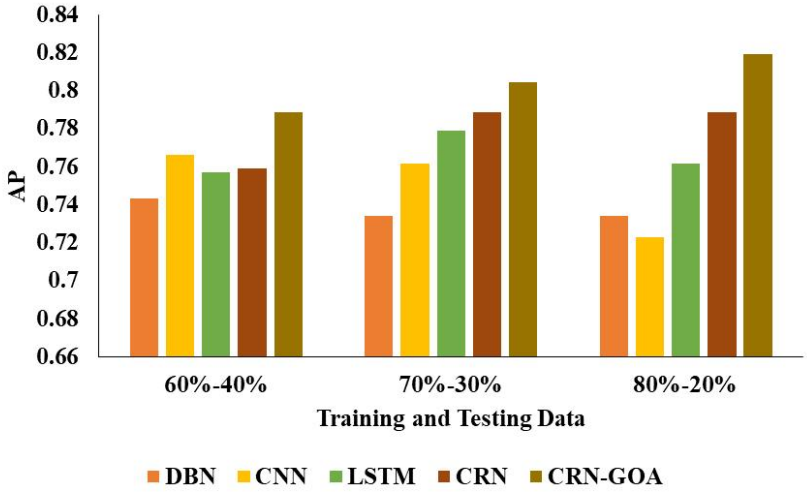

Figure 7. Comparison Analysis of AP

4.2 Comparison Analysis of Binary and Multi-class Classification

In this section, the presentation analysis of projected model is tested with binary and multiclass classification. Here the binary includes whether the patient is normal or abnormal to do the ADL and multiclass includes three classes. Table 4 and 5 present the exhibition analysis of projected model with existing techniques.

Table 4. Analysis of Proposed Model for Multiclass Classification

Classifiers	Accuracy	Precision	Recall	F1score
DBN	0.8864 ± 0.0028	0.8604 ± 0.0032	0.8748 ± 0.0041	0.8675 ± 0.0032
CNN	0.8977 ± 0.0033	0.8693 ± 0.0055	0.8890 ± 0.0029	0.8790 ± 0.0040
LSTM	0.7197 ± 0.0025	0.6364 ± 0.0044	0.6730 ± 0.0038	0.6542 ± 0.0034
CRN	0.8335 ± 0.0020	0.7870 ± 0.0029	0.8158 ± 0.0030	0.8011 ± 0.0024
CRN-GOA	0.9021 ± 0.0039	0.8941 ± 0.0047	0.8778 ± 0.0049	0.8859 ± 0.0046

Table 5. Analysis of Proposed Model for Binary Classification

Classifiers	Accuracy	Precision	Recall	F1 Score
DBN	0.8933 ± 0.0029	0.8656 ± 0.0039	0.8795 ± 0.0037	0.8725 ± 0.0035
CNN	0.8990 ± 0.0063	0.8791 ± 0.0065	0.8833 ± 0.0079	0.8812 ± 0.0069
LSTM	0.7355 ± 0.0028	0.6453 ± 0.0047	0.6850 ± 0.0045	0.6646 ± 0.0038
CRN	0.8438 ± 0.0064	0.8004 ± 0.0095	0.8254 ± 0.0072	0.8127 ± 0.0081
CRN-GOA	0.9179 ± 0.0044	0.9083 ± 0.0059	0.8917 ± 0.0057	0.8992 ± 0.0053

Above tables represent the Analysis of Proposed Model for Multiclass classification. In this analysis, different classifiers were utilized. In DBN reached the accuracy of 0.8864 ± 0.0028, the precision rate of 0.8604 ± 0.0032, the recall value of 0.8748 ± 0.0041 and finally F1 score of 0.8675 ± 0.0032. CNN reached the accuracy of 0.8977 ± 0.0033, the precision rate of 0.8693 ± 0.0055, the recall value of 0.8890 ± 0.0029 and finally F1 score of 0.8790 ± 0.0040. LSTM reached the accuracy of 0.7197 ± 0.0025, the precision rate of 0.6364 ± 0.0044, the recall value of 0.6730 ± 0.0038 and finally F1 score of 0.6542 ± 0.0034. CRN reached the accuracy of 0.8335 ± 0.0020, the precision rate of 0.7870 ± 0.0029, the recall value of 0.8158 ± 0.0030 and finally F1 score of 0.8011 ± 0.0024. CRN-GOA reached the accuracy of 0.9021 ± 0.0039, the precision rate of 0.8941 ± 0.0047, the recall value of 0.8778 ± 0.0049 and finally F1 score of 0.8859 ± 0.0046 respectively.

Table 5 represents that the Analysis of Proposed Model for Binary classification. In this comparison analysis, the DBN reached the accuracy of 0.8933 ± 0.0029, precision of 0.8656 ± 0.0039, recall of 0.8795 ± 0.0037 and finally the F1 score of 0.8725 ± 0.0035. CNN reached the accuracy of 0.8990 ± 0.0063, the precision of 0.8791 ± 0.0065, the recall of 0.8833 ± 0.0079 and finally the F1 score of 0.8812 ± 0.0069. LSTM reached 0.7355 ± 0.0028, the precision of 0.6453 ± 0.0047, the reached the recall of 0.6850 ± 0.0045 and finally the F1 score of 0.6646 ± 0.0038. CRN reached the accuracy of 0.8438 ± 0.0064, the precision of 0.8004 ± 0.0095, the reached the recall of 0.8254 ± 0.0072 and finally the F1 score of 0.8127 ± 0.0081. The proposed model CRN-GOA reached the accuracy of 0.9179 ± 0.0044, the precision of 0.9083 ± 0.0059, the recall of 0.8917 ± 0.0057 and finally the F1 score of 0.8992 ± 0.0053 respectively.

4.3 Comparative Analysis of Proposed Optimization

In order to identify the performance of GOA, it must be verified with existing optimization models and it is given in Table 6. The compared techniques are tested with CRN for validation analysis and averaged results are presented in Table 6.

Table 6. Analysis of Proposed Optimizer with CRN

Optimization Analysis	Accuracy	F1-Score	Precision	Recall	AUC
Differential evolution (DE)	0.8690	0.8113	0.8713	0.8713	0.85
Salp swarm algorithm (SSA)	0.8735	0.8506	0.8847	0.8867	0.80
Arithmetic optimization algorithm	0.8624	0.8545	0.8755	0.8755	0.69

Optimization Analysis	Accuracy	F1-Score	Precision	Recall	AUC
(AOA)					
Butterfly	0.8400	0.8427	0.8428	0.8427	0.83
Water strider algorithm (WSA)	0.8241	0.8069	0.7778	0.8383	0.84
GOA	0.9171	0.8693	0.8927	0.9063	0.90

In the analysis of accuracy, the existing models such as DE, SSA, AOA, Butterfly, WSA achieved nearly 84% to 87%, where the GOA has 91%. The reason is that the GOA does not easily fall into local optimum. In the test analysis, the proposed GOA achieved 86% of F-score, 89% of precision, 90$ of recall and 90% of AUC, whereas the existing models achieved nearly 80% to 85% of F1-score, 83% to 88% of precision, recall and AUC. Figure 8 presents the graphical analysis of various optimization models.

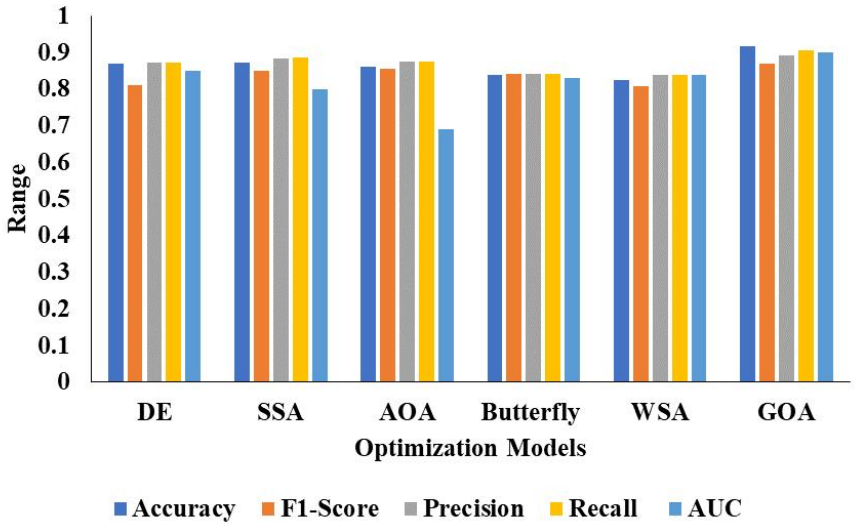

Figure 8. Analysis of Various Optimization Models with CRN

4.4 Ablation Study Analysis

In this section, the experiments are carried out to test the efficiency of proposed model by varying the epochs with three different learning rates, and it is mentioned in Table 7.

Table 7. Analysis of the Proposed Model by Varying the Learning Rate with Different Epochs

Learning Rate	Epoch	Accuracy	Precision	Recall	F1 Score	AUC
0.0003	10	77.2	26.2	74.9	38.9	84.2
	20	78.7	28.1	76.9	41.1	85.1
	30	79.8	28.7	73.3	41.2	86.3
	40	82.3	31.2	68.6	42.9	87.1
	50	82.3	31.3	69.3	43.2	87.6
	60	82.7	31.8	68.6	43.4	87.7
	70	81.3	30.1	70.6	42.2	87.6
	80	82.5	31.9	71.3	44.0	88.0
0.0001	10	80.7	29.9	73.9	42.6	87.2
	20	80.5	29.9	75.6	42.8	88.3
	30	80.8	30.1	74.9	43.0	88.0
	40	85.8	37.0	66.3	47.5	88.2
	50	89.7	47.2	53.1	50.0	86.2
	60	88.4	43.2	64.4	51.7	87.9
	70	86.1	37.4	64.0	47.2	87.3

Learning Rate	Epoch	Accuracy	Precision	Recall	F1 Score	AUC
	80	88.8	43.9	54.1	48.4	85.0
0.001	10	84.5	35.2	71.3	47.1	88.1
	20	84.7	35.1	68.0	46.3	86.9
	30	90.0	47.9	41.6	44.5	83.8
	40	89.1	44.6	52.1	48.1	80.4
	50	90.7	53.3	34.3	41.8	74.5
	60	89.6	46.2	42.6	44.3	78.3
	70	88.6	42.1	47.2	44.5	79.4
	80	88.7	42.5	46.5	44.4	77.5

When the learning rate is 0.0003, the accuracy of the proposed model is much less, i.e., 77% to 82% for 10 to 80 epochs, where the proposed model achieved 81% to 88% of accuracy on 0.0001 of learning rate and finally, it reached 89% to 91% of accuracy on 0.001 of learning rate. From this analysis, it is clearly proven that the learning rate plays a major role in the performance of proposed model. From the analysis, it is mentioned that the overfitting of the proposed model is up to the satisfactory level, hence in future work, it may be resolved by adding the propagation model for training. Figure 9 to 11 presents the graphical analysis of a proposed model for various learning rates.

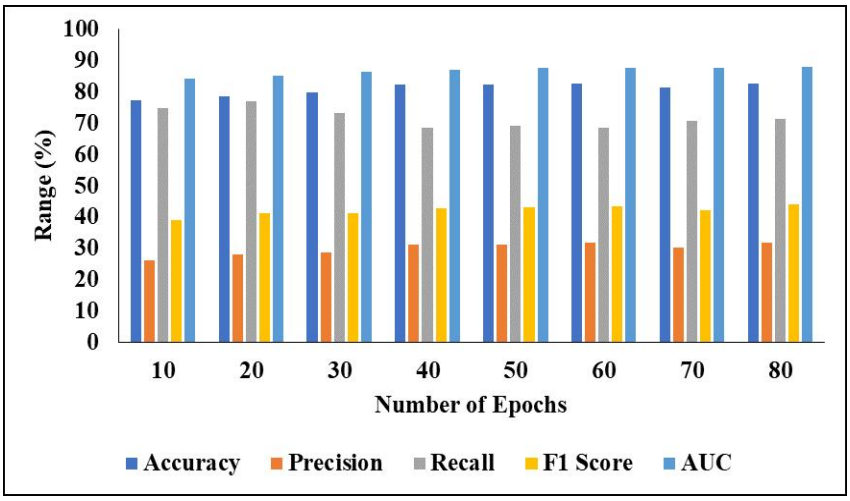

Figure 9. Analysis of Proposed Model for Learning Rate 0.0003

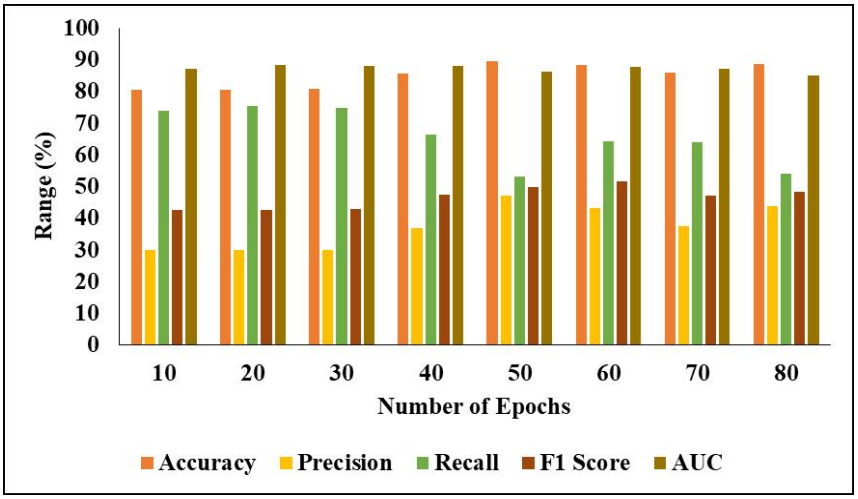

Figure 10. Performance of Proposed Model for Learning Rate 0.001

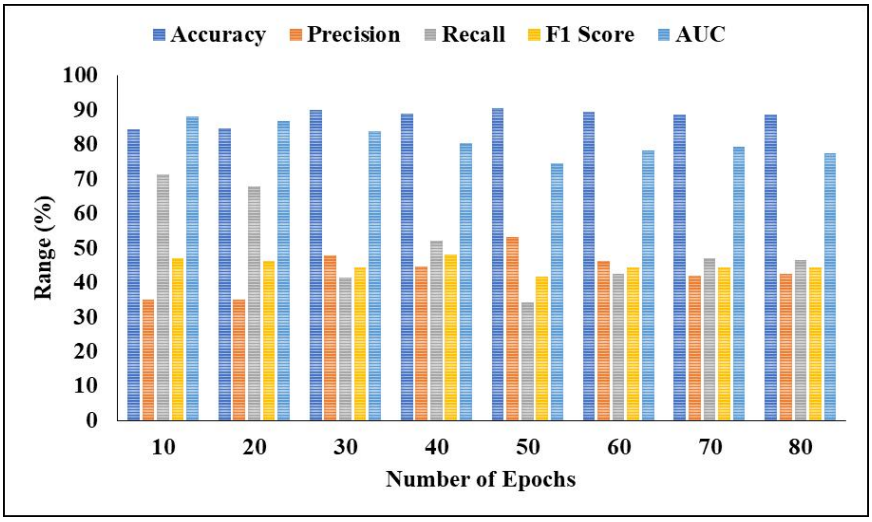

Figure 11. Comparative Analysis for Learning Rate 0.001

5. Conclusion

In this study, an improved deep learning model is used to evaluate BADL and IADL skills. In this paper, a new technique is presented for categorising ADL called CRN. To do this, an SRE module is created that explicitly learns class-wise feature illustrations by introducing a map. Also, the study introduced the attention loss as an auxiliary loss for CRN training to facilitate the acquisition of semantic knowledge about classes by the SRE module and CRN. The BADL and IADL of older Chinese were separated into three groups that comprised the largest group across all BADL/IADL scale items. Incredibly, a U-shaped relationship was found between age and functional impairment, and between body mass index and functional impairment. In the analysis of the test, the proposed model achieved 88% of accuracy, whereas the existing models such as CNN, LSTM and CRN achieved nearly 82% to 86% of accuracy for the 80%-20% of training and testing data. In addition, the performance analysis of GOA is also tested with other meta-heuristic approaches on CRN model to test its efficiency. In this work, it focused only on the elderly people of China, since most of the younger people's activities also lead to crime. The proposed model will be enhanced in future study to detect the ambulatory behaviours of the Chinese elderly as well as identify the behaviour of young people that leads to crime.

References

[1] M. Zerkouk, and Chikhaoui, B., "Spatio-temporal Abnormal Behavior Prediction in Elderly Persons Using Deep Learning Models," *Sensors*, vol. 20, no. 8, p. 2359, 2020.

[2] I. Mishkhal, S. A. A. Kareem, Saleh, H. H. and Alqayyar, A., "Deep Learning with network of Wearable sensors for preventing the Risk of Falls for Older People," In *IOP Conference Series: Materials Science and Engineering*, IOP Publishing, vol. 928, no. 3, p. 032050, 2020.

[3] M. F. Khan, Ghazal, T. M., Said, R. A., Fatima, A., Abbas, S., Khan, M. A., Issa, G. F., Ahmad, M. and Khan, M. A., "An Iomt-enabled Smart Healthcare Model to Monitor Elderly People Using Machine Learning Technique," *Computational Intelligence and Neuroscience*, 2021.

[4] W. Taylor, K. Dashtipour, Shah, S. A., Hussain, A., Abbasi, Q. H. and Imran, M. A., "Radar Sensing for Activity Classification in Elderly People Exploiting Micro-doppler Signatures Using Machine Learning," *Sensors*, vol. 21, no. 11, p. 3881, 2021.

[5] R. L. Priya, and Jinny, S. V., "Elderly Healthcare System for Chronic Ailments Using Machine Learning Techniques-A Review," *Iraqi Journal of Science*, vol. 62, no. 9, pp. 3138-3151, 2021.

[6] D. Flores-Martin, Rojo, J., Moguel, E., Berrocal, J. and Murillo, J.M., "Smart Nursing Homes: Self-management Architecture Based on Iot and Machine Learning for Rural Areas," *Wireless Communications and Mobile Computing*, pp.1-15, 2021.

[7] M. Gao, N. I. F. M. Noh and Lin, N.J., "Study on Carbon Emission Strategies of Rural Land Consolidation from the Perspective of Sustainable Energy Development," *Educational Administration: Theory and Practice*, vol. 29, no. 1, pp.269-276, 2023.

[8] X. Yu, H. Qiu, and S. Xiong, "A novel hybrid deep neural network to predict pre-impact fall for older people based on wearable inertial sensors," *Frontiers in bioengineering and biotechnology*, vol. 8, p.63, 2020.

[9] S. H. Yoon, "Educational Outcomes of After-School Programs in Korea: A Meta-Analysis," *Educational Administration: Theory and Practice*, vol. 29, no. 1, pp. 29-42, 2023.

[10] Y. A. Choi, S. J. Park, J. A. Jun, C. S. Pyo, K. H. Cho, H. S. Lee, and J. H. Yu, "Deep learning-based stroke disease prediction system using real-time bio signals," *Sensors*, vol. 21, no. 13, p.4269, 2021.

[11] Y. Nan, N. H. Lovell, Redmond, S. J., Wang, K., Delbaere, K. and van Schooten, K. S., "Deep learning for activity recognition in older people using a pocket-worn smartphone," *Sensors*, vol. 20, no. 24, p.7195, 2020.

[12] J. L. Speiser, K. E. Callahan, D. K. Houston, J. Fanning, T. M. Gill, J. M. Guralnik, A. B. Newman, M. Pahor, W. J. Rejeski and M. E. Miller, "Machine Learning in Aging: an Example of Developing Prediction Models for Serious Fall Injury in Older Adults," *The Journals of Gerontology: Series A*, vol. 76, no. 4, pp. 647-654, 2021.

[13] U. K. Sridevi, S. Sudhir, and Palaniappan, S., "Elderly behavior prediction using a deep learning model in smart homes," In *Applications of Deep Learning and Big IoT on Personalized Healthcare Services, IGI Global*, pp. 115-131, 2020.

[14] R. Zhu, Lv, Y., Wang, Z. and Chen, X., "Prediction of the hypertension risk of the elderly in built environments based on the LSTM deep learning and bayesian fitting method," *Sustainability*, vol. 13, no. 10, p.5724, 2021.

[15] D. Mukherjee, R. Mondal, P. K. Singh, R. Sarkar and D. Bhattacharjee, "EnsemConvNet: a deep learning approach for human activity recognition using smartphone sensors for healthcare applications," *Multimedia Tools and Applications*, vol. 79, pp. 31663-31690, 2020.

[16] B. Friedrich, S. Lau, L. Elgert, J. M. Bauer and A. Hein, "A Deep Learning Approach for TUG and SPPB Score Prediction of (Pre-) Frail Older Adults on Real-Life IMU Data," *Healthcare*, vol. 9, no. 2, p. 149, 2021.

[17] R. Aznar-Gimeno, G. Labata-Lezaun, A. Adell-Lamora, D. Abadía-Gallego, R. del-Hoyo-Alonso and C. González-Muñoz, "Deep learning for walking behaviour detection in elderly people using smart footwear," *Entropy*, vol. 23, no. 6, p.777, 2021.

[18] D. Bhattacharya, D. Sharma, W. Kim, M. F. Ijaz and P. K. Singh, "Ensem-HAR: An Ensemble Deep Learning Model for Smartphone Sensor-based Human Activity Recognition for Measurement of Elderly Health Monitoring," *Biosensors*, vol. 12, no. 6, p. 393, 2022.

[19] F. M. Garcia-Moreno, M. Bermudez-Edo, E. Rodríguez-García, J. M. Pérez-Mármol, J. L. Garrido and M. J. Rodríguez-Fórtiz, "A Machine Learning Approach for Semi-automatic Assessment of IADL Dependence in Older Adults with Wearable Sensors," *International Journal of Medical Informatics*, vol. 157, p. 104625, 2022.

[20] K. A. Alaghbari, M. H. M. Saad, Hussain, A. and Alam, M. R., "Activities recognition, anomaly detection and next activity prediction based on neural networks in smart homes," *IEEE Access*, vol. 10, pp. 28219-28232, 2022.

[21] V. R. Chifu, , Pop, C.B., Demjen, D., Socaci, R., Todea, D., Antal, M., Cioara, T., Anghel, I. and Antal, C., "Identifying and Monitoring the Daily Routine of Seniors Living at Home," *Sensors*, vol. 22, no.3, p. 992, 2022.

[22] B. Prenkaj, Aragona, D., Flaborea, A., Galasso, F., Gravina, S., Podo, L., Reda, E. and Velardi, P., "A self-supervised algorithm to detect signs of social isolation in the elderly from daily activity sequences," *Artificial Intelligence in Medicine*, vol. 135, p.102454, 2023.

[23] A. Peimankar, Winther, T.S., Ebrahimi, A. and Wiil, U.K., "A Machine Learning Approach for Walking Classification in Elderly People with Gait Disorders," *Sensors*, vol. 23, no.2, p.679, 2023.

[24] H. L. Chan, Ouyang, Y., Chen, R. S., Lai, Y.H., Kuo, C. C., Liao, G. S., Hsu, W. Y. and Chang, Y. J., "Deep neural Network for the Detections of Fall and Physical Activities Using Foot Pressures and inertial sensing," *Sensors*, vol. 23, no. 1, p. 495, 2023.

[25] P Kulurkar, C. K. Dixit, V.C. Bharathi, A. Monikavishnuvarthini, A. Dhakne, and P. Preethi, "AI Based Elderly Fall Prediction System Using Wearable Sensors: A Smart Home-care Technology with IOT," *Measurement: Sensors*, vol. 25, p.100614, 2023.

[26] Y. Zeng, W. V. James, Z. Xiao, C. Zhang, and Y. Liu, "Sociodemographic and Health Profiles of the Oldest Old in China," *Popul Dev Rev*, vol. 28, no.2, pp. 251-73, 2002.

[27] Y. Zeng, D. L. Poston, and D. A. Vlosky, "Healthy Longevity in China: Demographic, Socioeconomic, and Psychological Dimensions," Germany: Springer, 2008.

[28] H. Zhang, Y. Wang , D. Wu, and J. Chen, "Evolutionary Path of Factors Influencing Life Satisfaction among Chinese Elderly: A Perspective of Data Visualization," *Int J Environ Res Public Health*, vol. 3, p. 35, 2018.

[29] Q. Zhang, Y. Wu, T. Han, and E. Liu, "Changes in cognitive function and risk factors for cognitive impairment of the elderly in China: 2005-2014," *Int J Environ Res Public Health*, vol. 16, no. 16, p. 2847, 2019.

[30] J. O. Agushaka, A.E. Ezugwu, and L. Abualigah, "Gazelle Optimization Algorithm: A novel nature-inspired metaheuristic optimizer," *Neural Computing and Applications*, pp.1-33, 2022.

[31] X. Lei, and C. Bai, "Cognitive function and mental health of elderly people in China: findings from 2018 Clhls survey," *China Popul Dev Stud*, vol. 3, pp. 343-51, 2020.